

PARTITIONING OF ENERGY AND THE DEGREE OF MELTING AND VAPORIZATION IN PLANETARY IMPACT PROCESSES, John D. O'Keefe, Department of Earth and Space Sciences, UCLA, Los Angeles, CA 90024 and Thomas J. Ahrens, Seismological Laboratory, Division of Geological and Planetary Sciences, California Institute of Technology, Pasadena, CA 91125.

The flow fields produced by the impact of a gabbroic anorthosite and iron meteoroids on a planet, modelled as a gabbroic anorthosite half space, at velocities of 5, 7.5, 15, 30 and 45 km/s were computed using the Eulerian finite difference formulation of Hageman and Walsh (1) and the equation-of-state, phase change, and rheological models for gabbroic anorthosite previously reported (2,3). From these flow calculations the partitioning of energy and the amount of melt and vapor produced were determined within a thermodynamic framework in which the entropy generated within a given mass element (cell) upon passage of the impact-induced shock wave determines whether the involved mass remains solid, melts, or vaporizes (4,5).

The partitioning of energy, at a series of late times in the impact-induced crater flow, when the stress wave magnitudes have decayed to a fraction of the compressive yield strength have been calculated for spherical iron and gabbroic anorthosite projectiles impacting gabbroic anorthosite (Fe→An and An→An respectively). These results have bearing on both the accretion and evolution of the terrestrial planets and a representative series of partitions at late times are shown in Figs. 1 and 2.

For both types of impact, most of the kinetic energy of the meteoroid is converted into internal energy residing in the planetary surface material. The fraction of meteoroid kinetic energy in internal energy ranges from 0.70 at 5 km/s to 0.85 at 30 km/s for the An→An impact, and 0.74 and 0.91 at these same speeds for the Fe→An impact. At low velocities (for both cases) most of the internal energy is produced by the plastic work resulting from a finite yield strength (approximately 0.5 at 5 km/s) whereas the balance of the internal energy is from shock heating. At high velocities (> 15 km/s) the internal energy is produced predominantly by shock heating, and the fraction due to plastic work is decreased to 0.38 and 0.27 for An→An and Fe→An impacts, respectively.

The relative fraction of the impact energy residing in the kinetic energy of the planetary surface ranges from 10 to 7% for the An→An impacts and 9 to 7% for the Fe→An impacts. Most of this energy resides in the ejecta. An implication of these results is that the energy consumed by plastic work in strong rocks would be available for conversion to kinetic energy and thus increase the amount at ejecta for weak rocks and unconsolidated regoliths.

The degree of melting and vaporization produced by impact was calculated by constructing the isentropes, passing through the energy and volume states at one atmosphere pressure, that correspond to incipient and complete melting and vaporization (4,5). The amount of melt for an An→An impact ranged from approximately 1.5 times the meteoroid volume at 7.5 km/s to 102 times the meteoroid volume at 45 km/s; for an Fe→An impact the volume ranged from approximately 5 times the meteoroid volume at 7.5 km/s to over 250 times the meteoroid volume at 45 km/s. For values of the similarity variable (6),

PARTITIONING OF ENERGY

O'Keefe, J. D. et al.

$$S \equiv \frac{\rho_m}{\rho_p} \left(\frac{V}{C_p} \right)^2 > 4 \quad (1)$$

both the volume of melt produced by the An→An and Fe→An impacts approximately lie in a single straight line whose slope is proportional to the meteoroid kinetic energy. Here $\rho_p = 2.94$ or 7.8 g/cm^3 is the density of the gabbroic anorthosite and iron meteorite, respectively, ρ_m is the planetary surface density, V is projectile velocity and C_p is the bulk sound velocity in the projectile. For values of the similarity variable less than 4, the relative amount of melting decreases and the slope is no longer proportional to the meteoroid kinetic energy. The volume of melt (V_{mt}) divided by the volume of the meteoroid (V_m) is closely fit by

$$\left(\frac{V_{mt}}{V_m} \right) = 2.5 S ; S \gtrsim 4 \quad (2)$$

Using Z-model scaling of Maxwell (7) and the melt volume-crater diameter, D , relation of Dence (8) for the earth Eqs. 1 and 2 imply

$$V_{mt} \propto \left(\frac{\rho_m}{\rho_p} \right) g^{0.56} D^{3.55}; S \gtrsim 4, \text{ where } g \text{ is surface gravity.} \quad (3)$$

Empirically, we observe that the post-impact volume of craters is a function D^α , where α is less than 3, for large craters. Thus, the volume of melt relative to the volume of the crater would increase with crater diameter at least as rapidly as $D^{0.55}$. This predicted relative increase in melting with crater diameter is observed in the terrestrial and inferred to occur in lunar craters. The present results also predict that the amount of melt for a given crater diameter is greater in planets that have higher values of surface gravity. This implies that more melt will be observed in large terrestrial craters than similar-sized lunar craters.

ACKNOWLEDGEMENTS: This research was supported under NASA Grant NSG 7129. Contribution No. 2861, Division of Geological and Planetary Sciences, California Institute of Technology.

REFERENCES: (1) Hageman, L. J. and Walsh, J. M. (1970) *Systems, Science and Software, Report 3SR-35, V. 1.* (2) O'Keefe, J. D. and Ahrens, T. J. (1975) *Proc. Lunar Sci. Conf. 6th*, 2831-2844. (3) O'Keefe, J. D. and Ahrens, T. J. (1976) *Proc. Lunar Sci. Conf. 7th*, 3007-3025. (4) Ahrens, T. J. and O'Keefe, J. D. (1972) *The Moon*, 4, 214-249. (5) Ahrens, T. J. and O'Keefe, J. D. (1977) *Proc. Symp. Planet. Cratering Mechanics*, in press. (6) Dienes, J. K. and Walsh, J. M. (1970) *High Velocity Impact Phenomena*, ed. by R. Kinslow, Academic Press, 46-104. (7) Maxwell, D. E. (1976) *Proc. Symp. Planet. Cratering Mechanics*, in press. (8) Dence, M. R. (1965) *Annals N.Y. Acad. Sci.*, 123, 941-969.

PARTITIONING OF ENERGY

O'Keefe, J. D. et al.

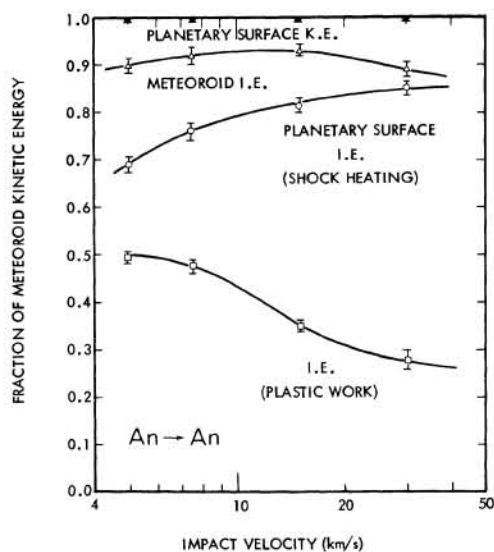


Fig. 1 Post-impact, energy partitioning for spherical gabbroic anorthosite object impacting gabbroic anorthosite half space versus impact velocity.

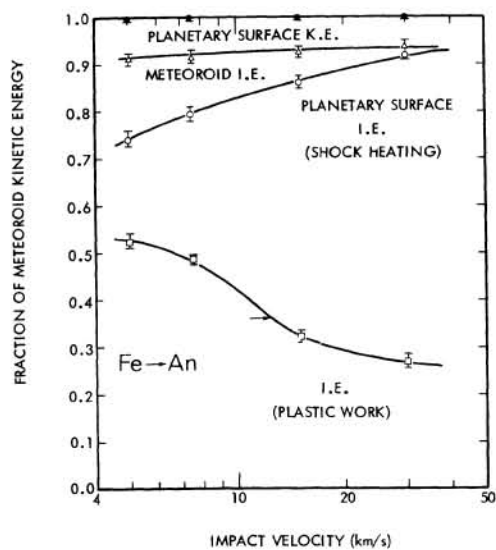


Fig. 2 Post-impact, energy partitioning for spherical iron object impacting gabbroic anorthosite half space versus impact velocity.

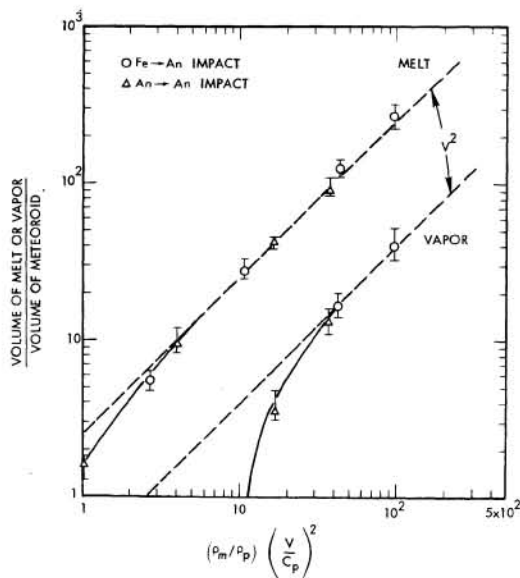


Fig. 3 Normalized melt volume and vapor volume, versus impact velocity similarity variable, S .